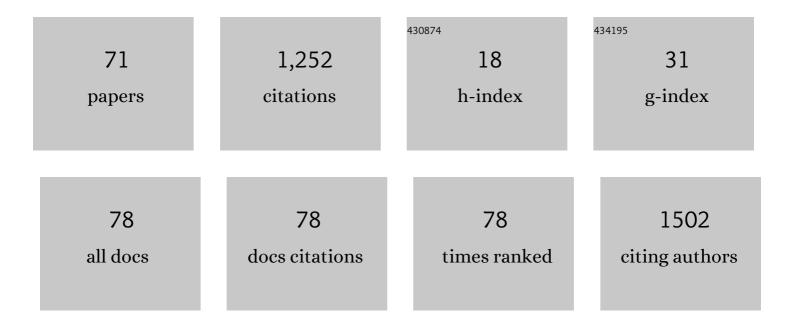
Elin TrägÃ¥rdh

List of Publications by Year in descending order

Source: https://exaly.com/author-pdf/5801496/publications.pdf Version: 2024-02-01



#	Article	IF	CITATIONS
1	Complete metabolic response with [¹⁸ F]fluorodeoxyglucoseâ€positron emission tomography/computed tomography predicts survival following induction chemotherapy and radical cystectomy in clinically lymph node positive bladder cancer. BJU International, 2022, 129, 174-181.	2.5	13
2	Deep learning takes the pain out of back breaking work - Automatic vertebral segmentation and attenuation measurement for osteoporosis. Clinical Imaging, 2022, 81, 54-59.	1.5	2
3	Freely available convolutional neural network-based quantification of PET/CT lesions is associated with survival in patients with lung cancer. EJNMMI Physics, 2022, 9, 6.	2.7	5
4	Relationship between somatostatin receptor expressing tumour volume and healthâ€related quality of life in patients with metastatic <scp>GEPâ€NET</scp> . Journal of Neuroendocrinology, 2022, 34, e13139.	2.6	2
5	Freely available artificial intelligence for pelvic lymph node metastases in PSMA PET-CT that performs on par with nuclear medicine physicians. European Journal of Nuclear Medicine and Molecular Imaging, 2022, 49, 3412-3418.	6.4	16
6	Artificial intelligenceâ€based detection of lymph node metastases by PET/CT predicts prostate cancerâ€specific survival. Clinical Physiology and Functional Imaging, 2021, 41, 62-67.	1.2	20
7	Automated Bone Scan Index as an Imaging Biomarker to Predict Overall Survival in the Zometa European Study/SPCG11. European Urology Oncology, 2021, 4, 49-55.	5.4	9
8	Assessment of Ventilation and Perfusion in Patients with COVID-19 Discloses Unique Information of Pulmonary Function to a Clinician: Case Reports of V/P SPECT. Clinical Medicine Insights: Circulatory, Respiratory and Pulmonary Medicine, 2021, 15, 117954842110301.	0.9	1
9	Head-to-head comparison of a Si-photomultiplier-based and a conventional photomultiplier-based PET-CT system. EJNMMI Physics, 2021, 8, 19.	2.7	3
10	Artificial intelligence-aided CT segmentation for body composition analysis: a validation study. European Radiology Experimental, 2021, 5, 11.	3.4	22
11	Tumor Detection of ¹⁸ F-PSMA-1007 in the Prostate Gland in Patients with Prostate Cancer Using Prostatectomy Specimens as Reference Method. Journal of Nuclear Medicine, 2021, 62, 1735-1740.	5.0	10
12	Al-based detection of lung lesions in [18F]FDG PET-CT from lung cancer patients. EJNMMI Physics, 2021, 8, 32.	2.7	18
13	Patterns of pathologic lymph nodes in anal cancer: a PET-CT-based analysis with implications for radiotherapy treatment volumes. BMC Cancer, 2021, 21, 447.	2.6	5
14	Post-reconstruction enhancement of [18F]FDG PET images with a convolutional neural network. EJNMMI Research, 2021, 11, 48.	2.5	8
15	Artificial intelligence could alert for focal skeleton/bone marrow uptake in Hodgkin's lymphoma patients staged with FDG-PET/CT. Scientific Reports, 2021, 11, 10382.	3.3	9
16	A retrospective study assessing the accuracy of [18F]–fluorocholine PET/CT for primary staging of lymph node metastases in intermediate and high-risk prostate cancer patients undergoing robotic-assisted laparoscopic prostatectomy with extended lymph node dissection. Scandinavian Journal of Urology, 2021, 55, 293-297.	1.0	3
17	Impact of the COVID-19 pandemic on nuclear medicine departments in Europe. European Journal of Nuclear Medicine and Molecular Imaging, 2021, 48, 3361-3364.	6.4	6
18	Artificial intelligence-based measurements of PET/CT imaging biomarkers are associated with disease-specific survival of high-risk prostate cancer patients. Scandinavian Journal of Urology, 2021, 55, 427-433.	1.0	2

Elin TrÃ**g**Ã¥rdh

#	Article	IF	CITATIONS
19	Dose-reduced [18F]PSMA-1007 PET is feasible for functional imaging of the renal cortex. EJNMMI Physics, 2021, 8, 70.	2.7	5
20	Automated artificial intelligence-based analysis of skeletal muscle volume predicts overall survival after cystectomy for urinary bladder cancer. European Radiology Experimental, 2021, 5, 50.	3.4	5
21	Assessing Radiographic Response to 223Ra with an Automated Bone Scan Index in Metastatic Castration-Resistant Prostate Cancer Patients. Journal of Nuclear Medicine, 2020, 61, 671-675.	5.0	18
22	Denoising of Scintillation Camera Images Using a Deep Convolutional Neural Network: A Monte Carlo Simulation Approach. Journal of Nuclear Medicine, 2020, 61, 298-303.	5.0	26
23	Deep learningâ€based quantification of PET/CT prostate gland uptake: association with overall survival. Clinical Physiology and Functional Imaging, 2020, 40, 106-113.	1.2	32
24	Auto-segmentations by convolutional neural network in cervical and anorectal cancer with clinical structure sets as the ground truth. Clinical and Translational Radiation Oncology, 2020, 25, 37-45.	1.7	13
25	Optimization of [18F]PSMA-1007 PET-CT using regularized reconstruction in patients with prostate cancer. EJNMMI Physics, 2020, 7, 31.	2.7	17
26	RECOMIA—a cloud-based platform for artificial intelligence research in nuclear medicine and radiology. EJNMMI Physics, 2020, 7, 51.	2.7	45
27	Impact of acquisition time and penalizing factor in a block-sequential regularized expectation maximization reconstruction algorithm on a Si-photomultiplier-based PET-CT system for 18F-FDG. EJNMMI Research, 2019, 9, 64.	2.5	29
28	The use of a proposed updated EARL harmonization of 18F-FDG PET-CT in patients with lymphoma yields significant differences in Deauville score compared with current EARL recommendations. EJNMMI Research, 2019, 9, 65.	2.5	27
29	Comparison of conventional and Si-photomultiplier-based PET systems for image quality and diagnostic performance. BMC Medical Imaging, 2019, 19, 81.	2.7	10
30	Impact of penalizing factor in a block-sequential regularized expectation maximization reconstruction algorithm for 18F-fluorocholine PET-CT regarding image quality and interpretation. EJNMMI Physics, 2019, 6, 5.	2.7	15
31	Artificial intelligenceâ€based versus manual assessment of prostate cancer in the prostate gland: a method comparison study. Clinical Physiology and Functional Imaging, 2019, 39, 399-406.	1.2	30
32	A Prospective Observational Study to Evaluate the Effects of Long-Acting Somatostatin Analogs on ⁶⁸ Ga-DOTATATE Uptake in Patients with Neuroendocrine Tumors. Journal of Nuclear Medicine, 2019, 60, 1717-1723.	5.0	25
33	Deep learning for segmentation of 49 selected bones in CT scans: First step in automated PET/CT-based 3D quantification of skeletal metastases. European Journal of Radiology, 2019, 113, 89-95.	2.6	96
34	Automated quantification of reference levels in liver andÂmediastinal blood pool for the Deauville therapy response classification using FDG-PET/CT in Hodgkin andÂnon-Hodgkin lymphomas. Clinical Physiology and Functional Imaging, 2019, 39, 78-84.	1.2	16
35	Comparison between silicon photomultiplier-based and conventional PET/CT in patients with suspected lung cancer—a pilot study. EJNMMI Research, 2019, 9, 35.	2.5	10
36	A prospective study to evaluate the intra-individual reproducibility of bone scans for quantitative assessment in patients with metastatic prostate cancer. BMC Medical Imaging, 2018, 18, 8.	2.7	2

Elin TrÃ**g**Ã¥rdh

#	Article	IF	CITATIONS
37	Evaluation of changes in Bone Scan Index at different acquisition timeâ€points in bone scintigraphy. Clinical Physiology and Functional Imaging, 2018, 38, 1015-1020.	1.2	4
38	3D skeletal uptake of 18F sodium fluoride in PET/CT images is associated with overall survival in patients with prostate cancer. EJNMMI Research, 2017, 7, 15.	2.5	33
39	Systematic review of cost-effectiveness of myocardial perfusion scintigraphy in patients with ischaemic heart disease. European Heart Journal Cardiovascular Imaging, 2017, 18, 825-832.	1.2	15
40	Association of PET index quantifying skeletal uptake in NaF PET/CT images with overall survival in prostate cancer patients Journal of Clinical Oncology, 2017, 35, 178-178.	1.6	0
41	Bone Scan Index as an Imaging Biomarker in Metastatic Castration-resistant Prostate Cancer: A Multicentre Study Based on Patients Treated with Abiraterone Acetate (Zytiga) in Clinical Practice. European Urology Focus, 2016, 2, 540-546.	3.1	27
42	A Preanalytic Validation Study of Automated Bone Scan Index: Effect on Accuracy and Reproducibility Due to the Procedural Variabilities in Bone Scan Image Acquisition. Journal of Nuclear Medicine, 2016, 57, 1865-1871.	5.0	31
43	Bone Scan Index and Progression-free Survival Data for Progressive Metastatic Castration-resistant Prostate Cancer Patients Who Received ODM-201 in the ARADES Multicentre Study. European Urology Focus, 2016, 2, 547-552.	3.1	13
44	Bone Scan Index as an imaging biomarker to predict overall survival in the Zeus/SPCG11 study Journal of Clinical Oncology, 2016, 34, e16599-e16599.	1.6	0
45	Perfusion vector—a new method to quantify myocardial perfusion scintigraphy images: a simulation study with validation in patients. EJNMMI Research, 2015, 5, 121.	2.5	2
46	Evaluation of inter-departmental variability of ejection fraction and cardiac volumes in myocardial perfusion scintigraphy using simulated data. EJNMMI Physics, 2015, 2, 2.	2.7	6
47	Reporting nuclear cardiology: a joint position paper by the European Association of Nuclear Medicine (EANM) and the European Association of Cardiovascular Imaging (EACVI). European Heart Journal Cardiovascular Imaging, 2015, 16, 272-279.	1.2	26
48	Computerized decision making in myocardial perfusion SPECT: The new era in nuclear cardiology?. Journal of Nuclear Cardiology, 2015, 22, 885-887.	2.1	4
49	Prevalence of manual Strauss LBBB criteria in patients diagnosed with the automated Glasgow LBBB criteria. Journal of Electrocardiology, 2015, 48, 558-564.	0.9	11
50	EANM procedural guidelines for radionuclide myocardial perfusion imaging with SPECT and SPECT/CT: 2015 revision. European Journal of Nuclear Medicine and Molecular Imaging, 2015, 42, 1929-1940.	6.4	260
51	Bone scan index as a biomarker to predict outcome in real-life mCRPC patients on abiraterone acetate: A multicenter study Journal of Clinical Oncology, 2015, 33, 217-217.	1.6	Ο
52	Bone Scan Index as a prognostic imaging biomarker during androgen deprivation therapy. EJNMMI Research, 2014, 4, 58.	2.5	28
53	Computer-aided diagnosis system outperforms scoring analysis in myocardial perfusion imaging. Journal of Nuclear Cardiology, 2014, 21, 416-423.	2.1	17
54	Area of ischemia assessed by physicians and software packages from myocardial perfusion scintigrams. BMC Medical Imaging, 2014, 14, 5.	2.7	6

4

Elin TrÃ**g**Ã¥rdh

#	Article	IF	CITATIONS
55	Increase in bone scan index during abiraterone treatment in relation to reduced survival in mCRPC patients Journal of Clinical Oncology, 2014, 32, 244-244.	1.6	0
56	When is reacquisition necessary due to high extra-cardiac uptake in myocardial perfusion scintigraphy?. EJNMMI Research, 2013, 3, 20.	2.5	9
57	Adding attenuation corrected images in myocardial perfusion imaging reduces the need for a rest study. BMC Medical Imaging, 2013, 13, 14.	2.7	14
58	Prognosis of patients without perfusion defects with and without rest study in myocardial perfusion scintigraphy. EJNMMI Research, 2013, 3, 58.	2.5	12
59	Nuclear medicine technologists are able to accurately determine when a myocardial perfusion rest study is necessary. BMC Medical Informatics and Decision Making, 2012, 12, 97.	3.0	3
60	Normal stress databases in myocardial perfusion scintigraphy – how many subjects do you need?. Clinical Physiology and Functional Imaging, 2012, 32, 455-462.	1.2	1
61	Referring physicians underestimate the extent of abnormalities in final reports from myocardial perfusion imaging. EJNMMI Research, 2012, 2, 27.	2.5	6
62	Small average differences in attenuation corrected images between men and women in myocardial perfusion scintigraphy: a novel normal stress database. BMC Medical Imaging, 2011, 11, 18.	2.7	4
63	High-frequency QRS electrocardiogram. Clinical Physiology and Functional Imaging, 2007, 27, 197-204.	1.2	8
64	Detection of acute myocardial infarction using the 12â€lead ECG plus inverted leads versus the 16â€lead ECG (with additional posterior and rightâ€sided chest electrodes). Clinical Physiology and Functional Imaging, 2007, 27, 368-374.	1.2	28
65	Reduced high-frequency QRS components in electrocardiogram leads facing an area of the heart with intraventricular conduction delay due to bundle branch block. Journal of Electrocardiology, 2007, 40, 127-132.	0.9	7
66	High-frequency electrocardiogram analysis in the ability to predict reversible perfusion defects during adenosine myocardial perfusion imaging. Journal of Electrocardiology, 2007, 40, 510-514.	0.9	9
67	How many ECG leads do we need?. Cardiology Clinics, 2006, 24, 317-330.	2.2	16
68	Determination of the ability of high-frequency ECG to estimate left ventricular mass in humans, determined by magnetic resonance imaging. Clinical Physiology and Functional Imaging, 2006, 26, 157-162.	1.2	4
69	Serial changes in the high-frequency ECG during the first year following acute myocardial infarction. Clinical Physiology and Functional Imaging, 2006, 26, 296-300.	1.2	4
70	Left ventricular mass by 12-lead electrocardiogram in healthy subjects: comparison to cardiac magnetic resonance imaging. Journal of Electrocardiology, 2006, 39, 67-72.	0.9	33
71	Reduced high-frequency QRS components in patients with ischemic heart disease compared to normal subjects. Journal of Electrocardiology, 2004, 37, 157-162.	0.9	32